***Vibrio cholerae* Arrests Intestinal Epithelial Proliferation through T6SS-dependent Activation of the Bone Morphogenetic Protein Pathway.**

AUTHORS:

Xinyue Xu[1], Edan Foley[1,2]*.

1. Department of Medical Microbiology and Immunology, Faculty of Medicine and Dentistry, University of Alberta, Edmonton, AB, Canada
2. Department of Cell Biology, Faculty of Medicine and Dentistry, University of Alberta, Edmonton, AB, Canada

*Corresponding Author: efoley@ualberta.ca

ABSTRACT

To maintain an effective barrier, intestinal epithelial progenitor cells must divide at a rate that matches the loss of dead and dying cells. Otherwise, epithelial breaches expose the host to systemic infection by gut-resident microbes. Unlike most pathogens, *Vibrio cholerae* blocks tissue repair by arresting progenitor proliferation in the *Drosophila* infection model. At present, we do not understand how *Vibrio* circumvents such a critical antibacterial defense. In a series of genetic experiments, we found that *V. cholerae* blocks epithelial repair by activating the growth inhibitor Bone Morphogenetic Protein (BMP) pathway in progenitors. Specifically, we discovered that interactions between *Vibrio* and gut commensals initiate BMP signaling via host innate immune defenses. Notably, we found that *Vibrio* also activates BMP and arrests proliferation in zebrafish intestines, indicating an evolutionarily conserved link between infection, BMP and failure in tissue repair. Combined, our study highlights how enteric pathogens engage host immune and growth regulatory pathways to disrupt intestinal epithelial repair.

INTRODUCTION

To maintain an effective barrier against harmful environmental agents, multipotent Intestinal Stem Cells (ISCs) divide at a pace that matches the loss of dying epithelial cells. For example, infectious microbes frequently induce host defenses that prompt the expulsion of damaged epithelial cells [1–5]. In response, ISCs divide at an accelerated rate to ensure an adequate supply of mature barrier cells[2–5]. Impaired epithelial renewal abates barrier function, allowing lumenal microbes to invade interstitial tissue, and promote disease. Thus, it is essential that we understand how enteric pathogens impact epithelial proliferation.

Vibrio cholerae (*Vc*) is a non-invasive, toxin-producing bacterium widely found in aquatic environments. Intestinal infection with *Vc* causes a variety of symptoms that range from mild gastrointestinal distress to the potentially fatal diarrheal disease, cholera. There are an estimated three million cholera cases with one hundred thousand deaths annually in endemic regions[6]. While antibiotics and vaccines protect from *Vc*, antibiotic-resistant strains are emerging, and current vaccines provide moderate, and time-limited protection[7]. Therefore, it is essential that we that we develop a complete molecular profile of the gut response to *Vc*.

The vinegar fly, *Drosophila melanogaster,* is a powerful system to study *Vc* pathogenesis[8]. Insects are natural *Vc* reservoirs and contribute to pathogen dissemination in endemic areas[9,10]. Like the vertebrate small intestine, the fly midgut epithelium exists as a monolayer maintained by multipotent ISCs that proliferate to generate a daughter stem cell and transient cell types that mature into absorptive enterocytes or secretory lineages[11–16]. Fly ISCs predominantly generate a committed enterocyte precursor known as the enteroblast (EB), and EB-ISC pairs are classically defined as the progenitor compartment. Flies infected with *Vc* develop cholera-like symptoms that include epithelial breaches and

watery diarrhea laden with live pathogens[17–19]. Like vertebrates, loss of cholera toxin does not completely abolish *Vc* virulence in flies, indicating that cholera toxin-independent mechanisms contribute to pathogenesis[17,18,20]. Flies have provided particularly valuable insights into the actions of *Vc* virulence factors. For example, polysaccharide-dependent biofilm formation allows *Vc* to colonize and persist in the fly gut[21]. The CtxA component of cholera toxin disrupts enterocyte junctions, leading to leakage, weight loss and reduced viability[22]. Furthermore, infection with *Vc* activates the fly Immune Deficiency (IMD) pathway[18,23], a key mediator of gut antibacterial defenses with extensive similarities to the vertebrate Tumor Necrosis Factor Receptor (TNFR) response[24,25]. *Vc*-dependent activation of IMD contributes to pathogenesis by blocking ISC proliferation and promoting delamination of damaged epithelial cells, effectively preventing barrier repair in infected hosts[18,19,23].

At present, it is unclear how IMD blocks proliferation, however a recent study showed that the *Vc* Type VI Secretion System (T6SS) is essential for arresting ISC division[26]. The T6SS is a syringe-like contractile apparatus that injects toxic effectors into susceptible prey, rapidly killing the target[27–30]. *Vc* uses the T6SS to eliminate competitors and enhance gut colonization[31–33]. T6SS-dependent killing of commensal bacteria contributes to *Vc* virulence, as inactivation of the T6SS or removal of gut commensals restores epithelial renewal, attenuates intestinal damage, and extends host lifespan after infection[19,26,34,35]. However, the underlying molecular mechanism of T6SS-dependent arrest of epithelial repair remains unclear.

Previously, we found that *Vc* enhances transcriptional expression of multiple Bone Morphogenetic Protein (BMP) pathway components in the fly progenitor compartment in a T6SS-dependent manner[5]. We consider this discovery noteworthy, as BMP members of the Transforming Growth Factor-β (TGF-β) cytokine family regulate intestinal homeostasis in flies and vertebrates[36–47]. In both systems, BMPs act in a paracrine manner to inhibit progenitor proliferation and promote intestinal epithelial cell

differentiation. Loss of BMP signaling in fly EBs leads to hyperproliferation of ISCs under normal conditions and upon infection with the entomopathogen *Erwinia carotovora carotovora 15* (*Ecc15*)[41].

In this study, we used *Drosophila* to determine if the *Vc* T6SS engages host BMP signaling to block intestinal epithelial renewal. We discovered that the T6SS is essential for BMP activation in progenitors, with indispensable contributions from commensal microbes and host IMD activity. Mechanistically, we showed that *Vc* specifically activates BMP in EBs, leading to a non-autonomous arrest of ISC proliferation. Together, our work resolves the mechanism by which *Vc* interacts with gut commensals and host innate defenses to prevent repair of the intestinal epithelial barrier. Notably, we extended this study to demonstrate that the T6SS also activates BMP and blocks ISC proliferation in a zebrafish infection model, suggesting an evolutionarily conserved impact of the T6SS on regeneration of damaged intestines.

RESULTS

The T6SS Induces BMP Activation in *Drosophila* Intestinal Progenitors.

In contrast to most enteric challenges, *Vc* causes widespread Intestinal Epithelial Cell (IEC) destruction without compensatory expansion of the progenitor pool[23,26]. At present, we do not understand how *Vc* blocks such an essential damage repair response. Recently, we showed that *Vc* enhances progenitor cell expression of multiple BMP pathway components in a T6SS-dependent fashion, including the ligand *decapentaplegic*, the type-I receptor *thickveins* (*tkv*), and the transcriptional target *spalt*[26]. As BMP is an evolutionarily conserved tumor suppressor that arrests IEC proliferation in flies and vertebrates, we tested the hypothesis that *Vc* prevents intestinal epithelial repair by activating BMP in progenitors.

In preliminary experiments, we used immunofluorescence-based imaging to determine the rostro-caudal distribution of GFP-expressing *Vc* in infected adult female midguts. We defined four levels of colonization that ranged from absent (level I) to extensive, biofilm-like accumulations (level IV, supplementary Figure S1A). We observed *Vc* distribution throughout the intestine, with prominent accumulations in the posterior midgut (supplementary Figure S1B), including IEC-associated *Vc* populations that had breached the peritrophic matrix (supplementary Figure S1C). As the posterior midgut is a region of high tissue turnover during damage, and *Vc* accumulates to the greatest extent in the posterior midgut, we elected to characterize relationships between *Vc,* BMP, and posterior midgut renewal in greater detail.

To determine if the T6SS activates BMP in host IECs, we quantified MAD phosphorylation (pMAD) in guts of uninfected $esg^{ts}/+$ flies, alongside $esg^{ts}/+$ flies that we challenged with the El Tor C6706 *Vc* strain, or the isogenic T6SS-deficient *vasK* deletion mutant (C6706Δ*vasK*)[48]. MAD phosphorylation provides a direct measure of BMP activation, and $esg^{ts}/+$ transgenic flies allow us to identify progenitors (small,

GFP-positive cells), enteroendocrine cells (Prospero (Pros)-positive and GFP-negative), and enterocytes (large, GFP and Pros-negative cells), effectively allowing us to quantify lineage-specific BMP activation (Figure 1A). Regardless of infection status, we observed a high incidence of BMP activation in Prospero-positive cells, indicating *Vc*-independent activation of BMP in the enteroendocrine lineage (Supplementary Figure 2). In contrast, we detected substantial, T6SS-specific impacts on BMP activation within the progenitor compartment. Uninfected *esg*^{ts}*/+* guts contained evenly spaced IECs with minimal BMP activation throughout the epithelium (Figures 1A-C). In agreement with earlier reports[19,26], challenges with C6706Δ*vasK* disrupted epithelial organization and prompted an expansion of GFP+ progenitor cell numbers (Figure 1A). We did not observe effects of C6706Δ*vasK* infection on MAD phosphorylation relative to uninfected controls (Figures 1A-C), suggesting that T6SS-deficient *Vc* fails to modify the host BMP pathway. Consistent with previous studies[23,26], we found that wild-type *Vc* caused extensive epithelial damage without an expansion of midgut progenitors (Figures 1A). However, and in contrast to T6SS-deficient *Vc*, the percentage of pMAD+ progenitors almost doubled in C6706-infected guts (Figures 1A-C). Combined with our earlier transcriptional profiles[26], our data indicate a T6SS-specific activation of BMP in the progenitor compartment with an accompanying failure to expand progenitor numbers during infection.

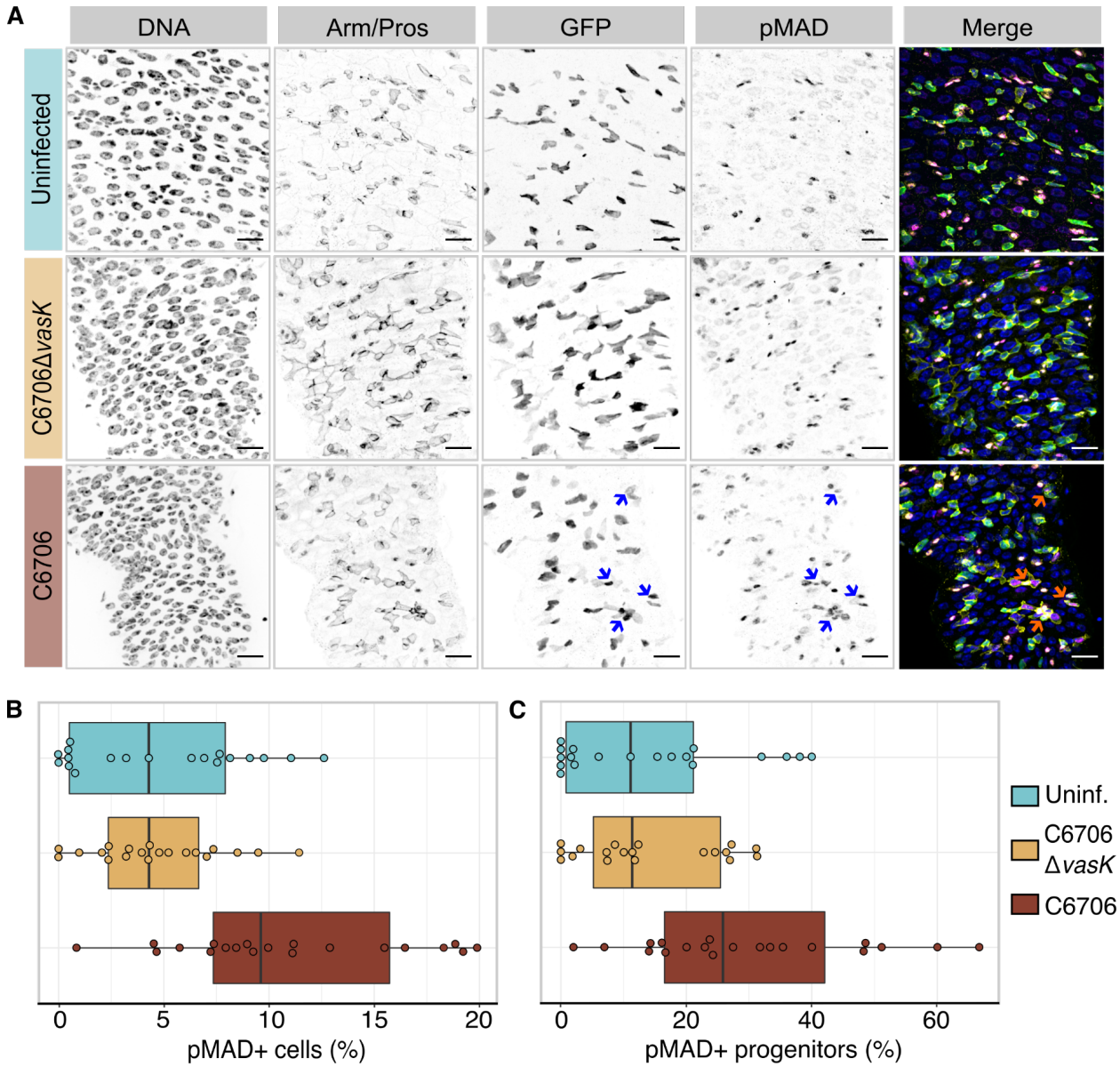

Test	ANOVA	Tukey	
P-value	2.26×10^{-5}	Uninf. vs Δ*vasK*	0.992
		Uninf. vs C6706	2×10^{-4}
		C6706 vs Δ*vasK*	1×10^{-4}

Test	ANOVA	Tukey	
P-value	9×10^{-4}	Uninf. vs Δ*vasK*	1.00
		Uninf. vs C6706	0.003
		C6706 vs Δ*vasK*	0.003

Figure 1. *Vc* activates BMP in intestinal progenitor cells in a T6SS-dependent manner. (A) Posterior midguts of *esg^{ts}/+* adult flies uninfected, infected with C6706Δ*vasK* or C6706 for 24 h. Hoechst labels DNA (blue), Armadillo and Prospero (Arm/Pros) label cell borders and enteroendocrine cells, respectively (yellow), GFP labels progenitors (green), and pMAD labels cells with BMP activation (magenta). Arrows = pMAD+ progenitors. Scale bars = 15 µm. **(B and C)** Percentage of **(B)** all cells or **(C)** progenitors that are pMAD+. Each dot represents a measurement from a single fly gut. P values are calculated using the significance tests indicated in tables.

Vc-Mediated Activation of BMP Requires Commensal Bacteria and Host Innate Defenses

As T6SS-dependent pathogenesis involves interactions between *Vc* and commensal bacteria in flies and mice[19,35], we asked if commensals are also required for T6SS-responsive BMP activation. In this instance, we quantified infection-dependent BMP activation in germ-free (GF) *esg*^{ts}*/+* flies relative to conventionally reared (CR) counterparts. We observed a significant increase in pMAD+ progenitor numbers of infected CR flies compared to uninfected controls (Figures 2B and 2C), with a parallel failure to increase progenitor numbers (Figures 2B and 2D), further supporting the argument that *Vc* activates BMP while arresting cell proliferation. We observed clear signs of epithelial damage in infected GF guts – loss of neatly organized cell borders, uneven internuclear spacing, and irregular distribution of GFP+ progenitors (Figure 2A). However, in the absence of gut-associated bacteria, infection significantly stimulated progenitor expansion (Figures 2A and 2D), without activation of BMP (Figures 2A and 2C), establishing a requirement for gut commensals to support *Vc*-dependent activation of BMP and arrest epithelial repair.

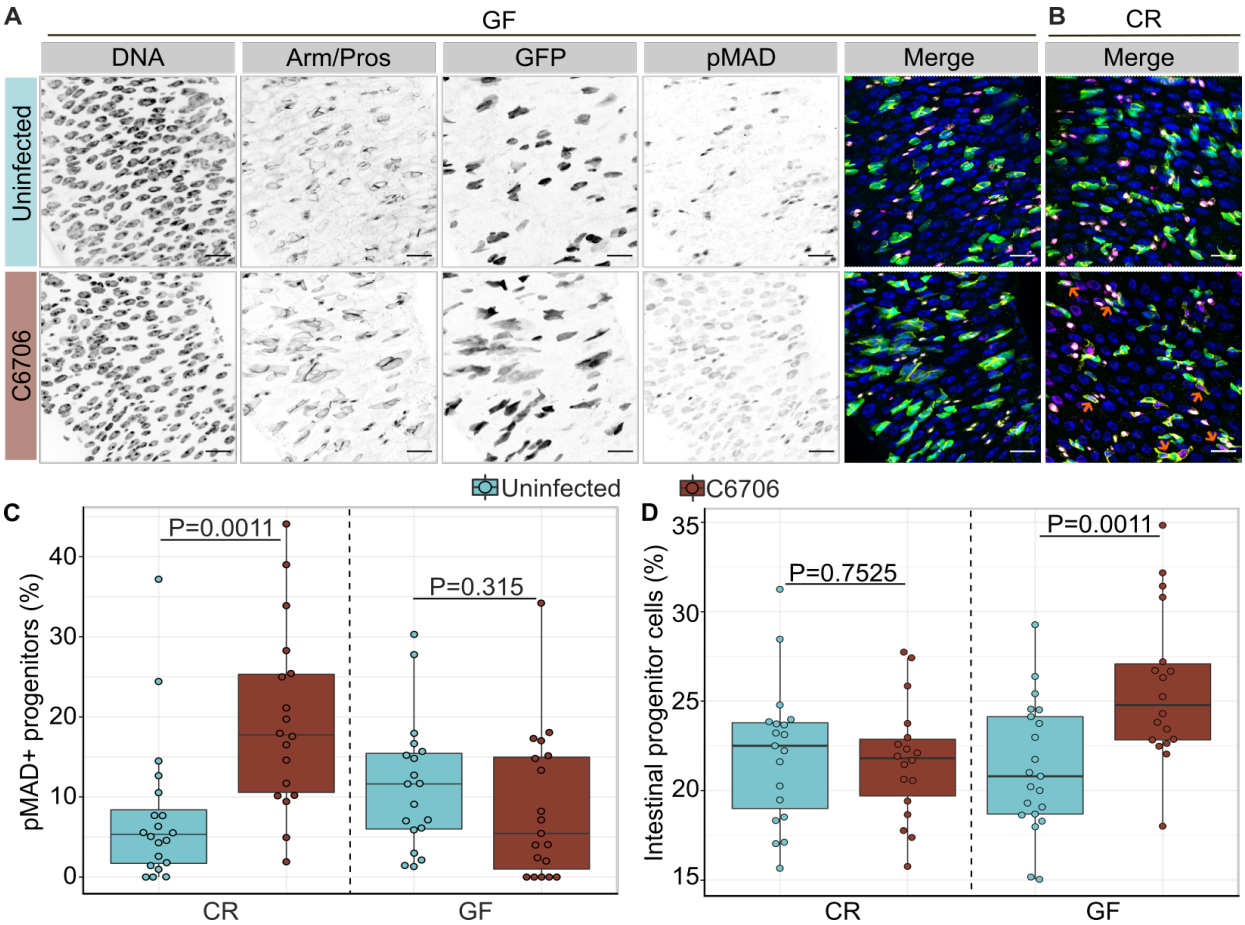

Figure 2. Progenitor-specific activation of BMP signaling requires *Vc*-commensal interactions. (A and B) Posterior midguts of **(A)** germ-free (GF) or **(B)** conventionally reared (CR) *esg*^{ts}*/+* adult flies uninfected or infected with C6706 for 24 h. Hoechst labels DNA (blue), Armadillo and Prospero (Arm/Pros) label cell borders and enteroendocrine cells, respectively (yellow), GFP labels progenitors (green), and pMAD labels cells with BMP activation (magenta). Scale bars = 15 µm. **(C)** Percentage of GFP+ progenitors that are pMAD+ in GF and CR *esg*^{ts}*/+* flies. **(D)** Proportion of GFP+ progenitors in all intestinal epithelial cells in GF and CR *esg*^{ts}*/+* flies. Each dot represents a measurement from a single fly gut. P values are calculated using unpaired Student t-tests.

As the TNFR-like Immune Deficiency (IMD) pathway orchestrates gut responses to commensal bacteria[3,49], and IMD prevents ISC proliferation upon *Vc* infection[19,23], we then asked if *Vc*-dependent intoxication of commensals activates BMP via IMD. To probe links between *Vc*, IMD, and BMP, we compared progenitor-specific BMP activation in wild-type and *imd* null mutant flies that we challenged with *Vc*. In agreement with Figures 1 and 2, we again found that *Vc* significantly increased the number of pMAD+ progenitors (small, Arm-enriched, Pros-negative cells) in wildtype host midguts (Figures 3A

and 3C). However, we also discovered that *Vc* failed to activate BMP in midguts of IMD-deficient flies (Figures 3B and 3C). As a whole, our data point to T6SS-dependent activation of progenitor cell BMP in a commensal and IMD-dependent manner.

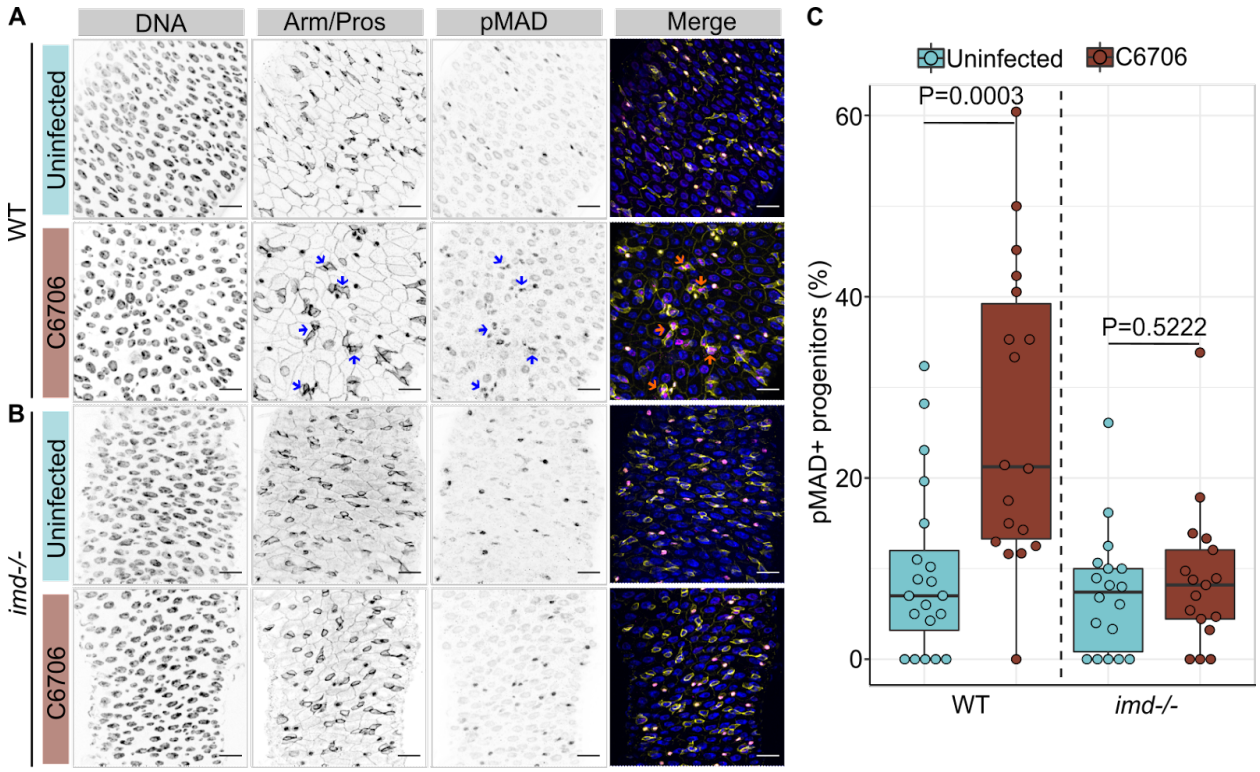

Figure 3. *Vc*-responsive activation of BMP requires IMD activity.
(A and B) Posterior midguts of **(A)** wild-type (WT) or **(B)** *imd* null mutant *(imd-/-*) adult flies uninfected or infected with C6706 for 24 h. Hoechst labels DNA (blue), Armadillo and Prospero (Arm/Pros) label cell borders and enteroendocrine cells, respectively (yellow), and pMAD labels cells with BMP activation (magenta). Arrows = pMAD+ progenitor cells. Scale bars = 15 µm. **(C)** Percentage of progenitors that are pMAD+ in WT and *imd-/-* flies. Each dot represents a measurement from a single fly gut. P values are calculated using unpaired Student t-tests.

Vc-Dependent Activation of BMP is Essential to Arrest Epithelial Repair in Infected Flies

Thus far, our data are consistent with a link between BMP activation by the T6SS and an arrest of progenitor cell expansion. However, we lack phenotypic data that specifically determines if BMP activation is essential for T6SS-dependent progenitor growth arrest. As T6SS-deficient *Vc* fail to activate

BMP or arrest progenitor expansion (e.g., Figure 1C), we first tested if progenitor-specific activation of BMP blocks ISC proliferation in flies challenged with T6SS-deficient *Vc*. Specifically, we compared progenitor cell expansion in control *esg*^{ts}*/+* flies and in flies that expressed a constitutively active variant of the type-I BMP receptor *tkv* (*esg*^{ts}*>tkv*^{CA}) in progenitors. We observed significant expansion of GFP+ progenitor cells in infected *esg*^{ts}*/+* guts, confirming activation of the host damage repair response (Figures 4A and 4C). In contrast, T6SS-deficient *Vc* failed to stimulate compensatory progenitor growth in *esg*^{ts}*>tkv*^{CA} guts (Figure 4B-C), demonstrating that progenitor-specific BMP activation is sufficient to arrest proliferation in an infected host.

In addition to preventing C6706Δ*vasK*-driven progenitor cell expansion, activation of the BMP pathway had visible effects on the intestinal epithelium of uninfected flies (Figure 4B), including a substantial decline in the number of intestinal progenitors (Figure 4C). Thus, while interesting, effects of *esg*^{ts}*>tkv*^{CA} on host responses to T6SS-deficient *Vc* do not adequately establish a requirement for BMP to arrest progenitor renewal after infection. To directly test if BMP modifies host responses to *Vc*, we specifically ablated BMP signaling in the progenitor compartment by knocking down the transcription factor *shn* (*esg*^{ts}*>shn*^{RNAi}) and monitored progenitor numbers in flies that we challenged with wild-type *Vc*. As anticipated, *Vc* did not stimulate compensatory progenitor growth in infected *esg*^{ts}*/+* flies (Figures 4D and 4F, Supplementary Figure 3). However, loss of BMP activity in progenitors effectively ablated *Vc*-mediated inhibition of progenitor growth. Instead, we found that infected *esg*^{ts}*>shn*^{RNAi} flies contained a significantly larger number of progenitors than their uninfected counterparts, similar to what we saw in wild-type guts upon challenge with T6SS-deficient *Vc* (Figures 4D-F). Together, these data demonstrate that BMP is necessary in the progenitor compartment to arrest epithelial renewal upon *Vc* infection.

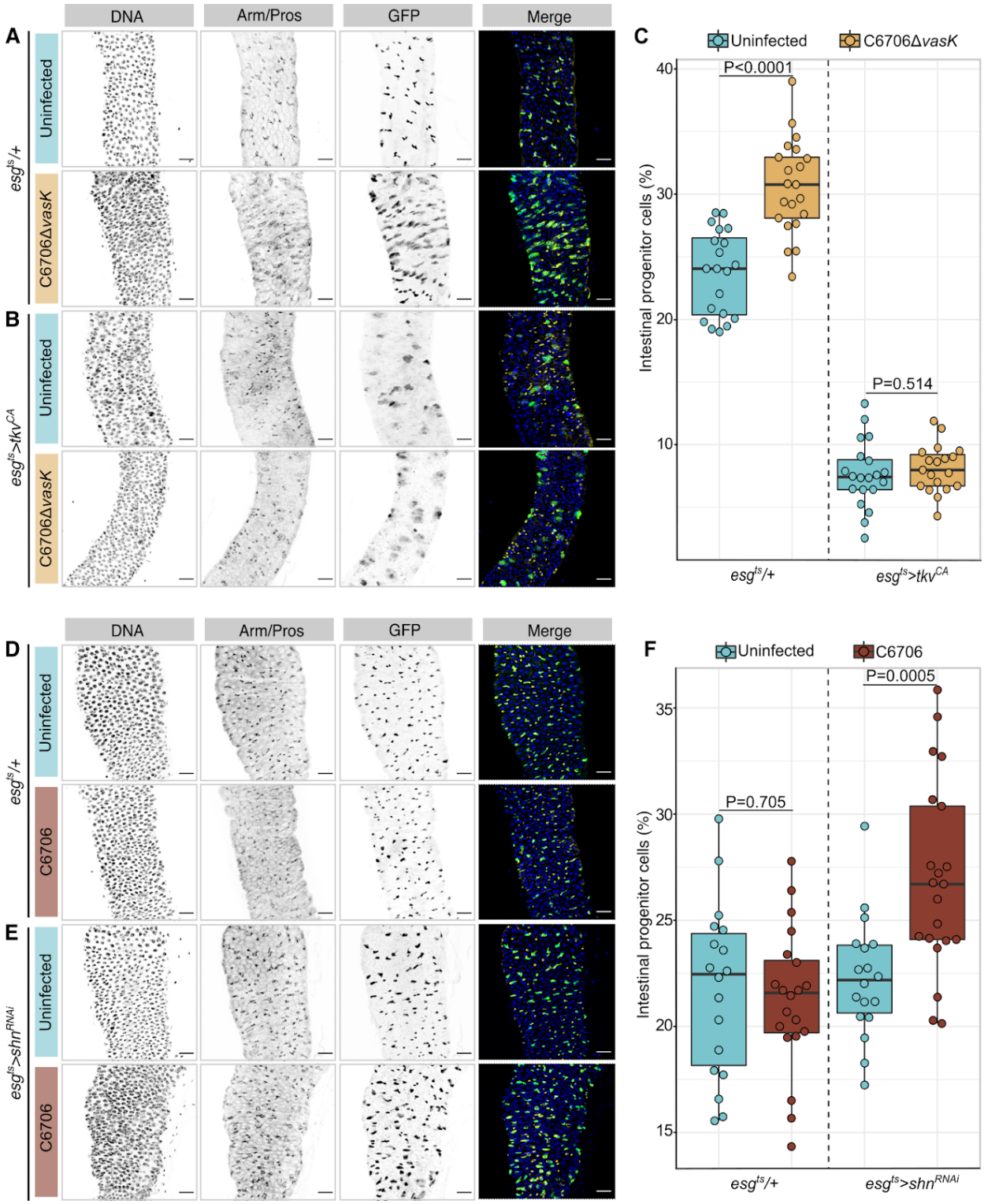

Figure 4. BMP regulates epithelial repair after *Vc* infection. (A and B) Posterior midguts from **(A)** wide-type (*esg^{ts}/+*) or **(B)** progenitor-specific BMP activation (*esg^{ts}>tkv^{CA}*) adult flies uninfected or infected with C6706Δ*vasK* for 36h. DNA labeled with Hoechst (blue), GFP marks progenitors (green), Armadillo (Arm) labels cell borders and Prospero (Pros) labels enteroendocrine cells (magenta). Scale bar = 25 µm. **(C)** Proportion of cells that are GFP+ progenitors in *esg^{ts}/+* and *esg^{ts}>tkv^{CA}* flies. Each dot represents a

measurement from a single fly gut. P values are calculated using unpaired Student t-tests. **(D and E)** Images of **(D)** wide-type (*esg^{ts}/+*) or **(E)** progenitor-specific BMP inhibition (*esg^{ts}>shn^{RNAi}*) adult flies uninfected or infected with C6706 for 36h. DNA labeled with Hoechst (blue), GFP marks progenitors (green), Armadillo (Arm) labels cell borders and Prospero (Pros) labels enteroendocrine cells (magenta). Scale bar = 25 µm. **(F)** Proportion of cells that are GFP+ progenitors in *esg^{ts}/+* and *esg^{ts}>shn^{RNAi}* flies. Each dot represents a measurement from a single fly gut. P values are calculated using unpaired Student t-tests.

BMP-dependent arrest of proliferation requires a non-autonomous signal from EBs to ISCs

As progenitor cells consist of self-renewing ISCs and transient EBs, we next identified the exact progenitor cell type required for BMP-dependent arrest of epithelial repair. To test if *Vc* activates BMP in a specific progenitor cell type, we challenged EB-specific driver line *Su(H)^{ts}/+* flies with C6706 and quantified the number of pMAD+ ISCs (Dl+, GFP-) and pMAD+ EBs (Dl-, GFP+) in the posterior midguts. In both infected and uninfected guts, there were similar and relatively low amounts of ISCs with BMP activity (Figures 5A and 5B). In contrast, infection with C6706 stimulated a more than threefold increase in the percentages of pMAD+ EBs (Figures 5A and 5B), indicating that *Vc* infection preferentially activates BMP in EBs. To test the impact of EB-specific BMP activation on epithelial renewal during infection, we knocked down *shn* exclusively in EBs (*Su(H)^{ts}>shn^{RNAi}*) and quantified progenitors after infection. We discovered that, like progenitor-wide knockdown, EB-specific loss of *shn* ablated *Vc*-responsive arrest of progenitor growth (Figure 5C). Specifically, the expansion of progenitors was a result of an increased population of ISCs not EBs (Figures 5D and 5E). Recent studies showed that inactivation of BMP in EBs induces ISC proliferation under homeostatic conditions or during bacterial infections [43]. Here, our results reveal that *Vc* infection primarily activates BMP in EBs, which blocks stem cell proliferation and therefore impairs epithelial renewal non-cell autonomously.

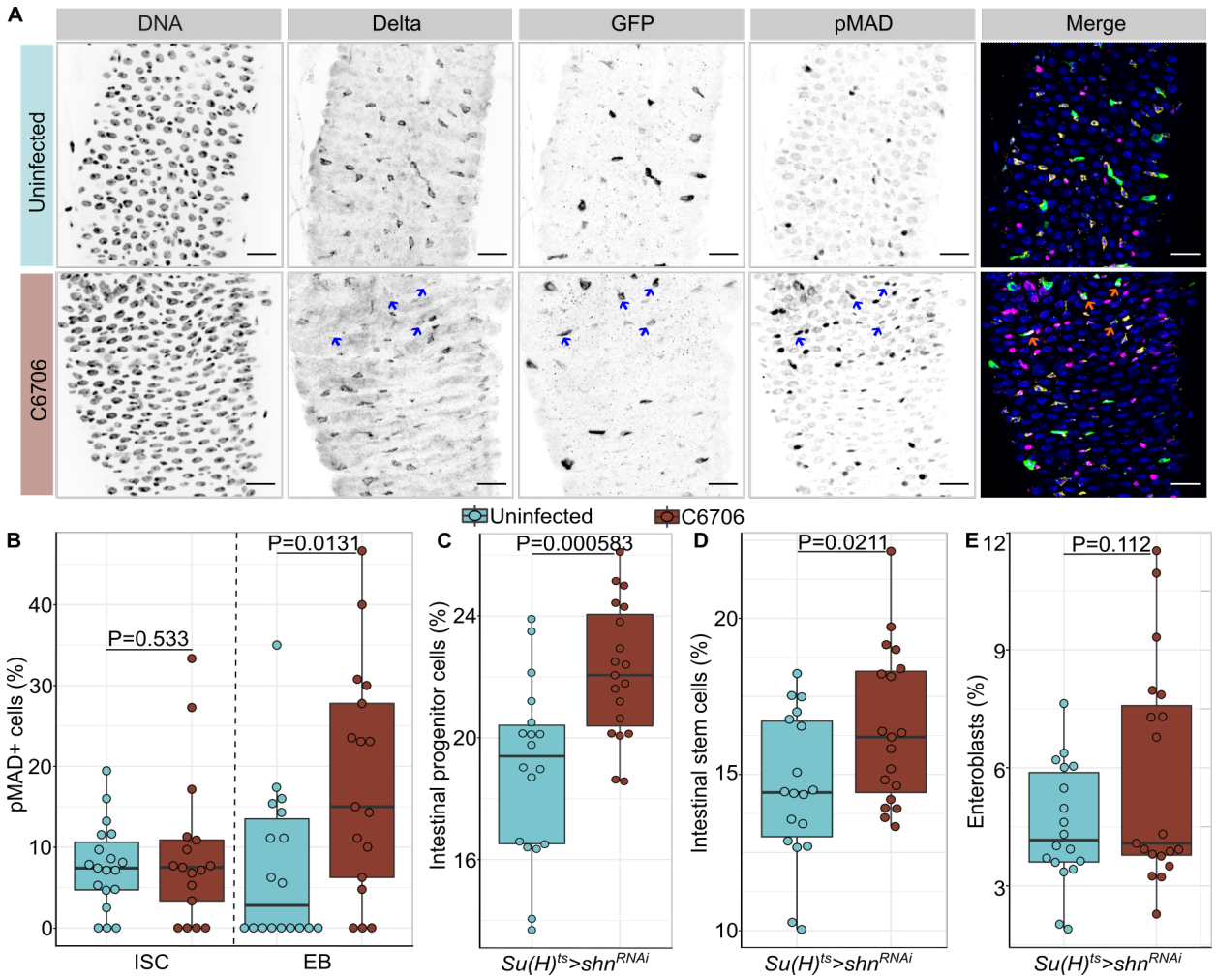

Figure 5. *Vc*-responsive BMP activation in EBs arrests intestinal stem cell growth non-cell autonomously. (A) Posterior midguts of uninfected or C6706 infected *Su(H)^{ts}/+* adult flies. DNA marked by Hoechst (blue), Delta+ intestinal stem cells (yellow), Su(H)+ EBs marked by GFP (green), and pMAD (magenta) to monitor BMP activation. Arrowheads = pMAD+ EBs. Scale bars = 15 µm. **(B)** Proportion of intestinal stem cells or EBs that are pMAD+ in *Su(H)^{ts}/+* intestines. **(C-E)** Proportions of all cells that are **(C)** progenitors, **(D)** intestinal stem cells, or **(E)** EBs in the intestines with EB-specific BMP inactivation (*Su(H)^{ts}>shn^{RNAi}*). Each dot represents a measurement from a single fly gut. P values are calculated using Student t-tests.

The T6SS suppresses cell proliferation and induces TGF-β/BMP activation in a vertebrate intestine.

To expand our study, we then asked if the impact of the *Vc* T6SS on intestinal epithelial renewal applies to vertebrate hosts. Zebrafish *Danio rerio* are ideal vertebrate models to study *Vc* pathogenesis[50–52]. Fish intestines are naturally colonized by *Vibrio* species and develop cholera-like symptoms upon *Vc* infection[50,52–55]. Importantly, like the mammalian intestine, the zebrafish intestinal epithelium contains

a complex community of secretory and absorptive lineages that interact with immune-regulatory myeloid and lymphoid cells[56,57]. To test whether the *Vc* T6SS impacts epithelial repair in fish, we challenged zebrafish larvae and adults with either wildtype *Vc* (C6706) or T6SS-deficient *Vc* (C6706Δ*vasK*) and measured cell proliferation. In larvae, uninfected intestines contained moderate amounts of EdU+ proliferating cells (Figures 6A and 6B). Infection with C6706Δ*vasK* promoted epithelial repair indicated by a significantly higher proliferation rate compared to uninfected guts (Figures 6A and 6B). In contrast, there was no significant difference in numbers of EdU+ cells between C6706-infected and uninfected guts. In parallel to our findings in larvae, we also discovered that the *Vc* T6SS disrupts IEC regeneration in adult zebrafish intestines. Both C6706 and C6706Δ*vasK* damaged the intestinal epithelium, characterized by disorganized IECs and lumenal shedding of damaged tissue (Figure 6C). Damage in C6706Δ*vasK*-infected guts stimulated repair, as the numbers of PCNA+ proliferating cells nearly doubled compared to uninfected counterparts (Figures 6C-D). In contrast, we did not detect significant changes in cell proliferation rates after C6706 infection (Figures 6C-D). These data demonstrate that, like a fly host, *Vc* arrests epithelial proliferation in zebrafish intestines in a T6SS-dependent manner. Furthermore, we found that *the* T6SS induced TGF-β/BMP, as larvae infected with wildtype *Vc* contained significantly larger numbers of cells with an active, phosphorylated form of SMAD3 (pSMAD3) compared to the uninfected and T6SS-deficient *Vc* infected counterparts (Figures 6E and 6F). Although further studies are needed to determine whether TGF-β/BMP activity is necessary for T6SS-responsive arrest of cell proliferation, our findings raise the possibility that *Vc* blocks intestinal epithelial repair upon damage through similar mechanisms in invertebrates and vertebrates.

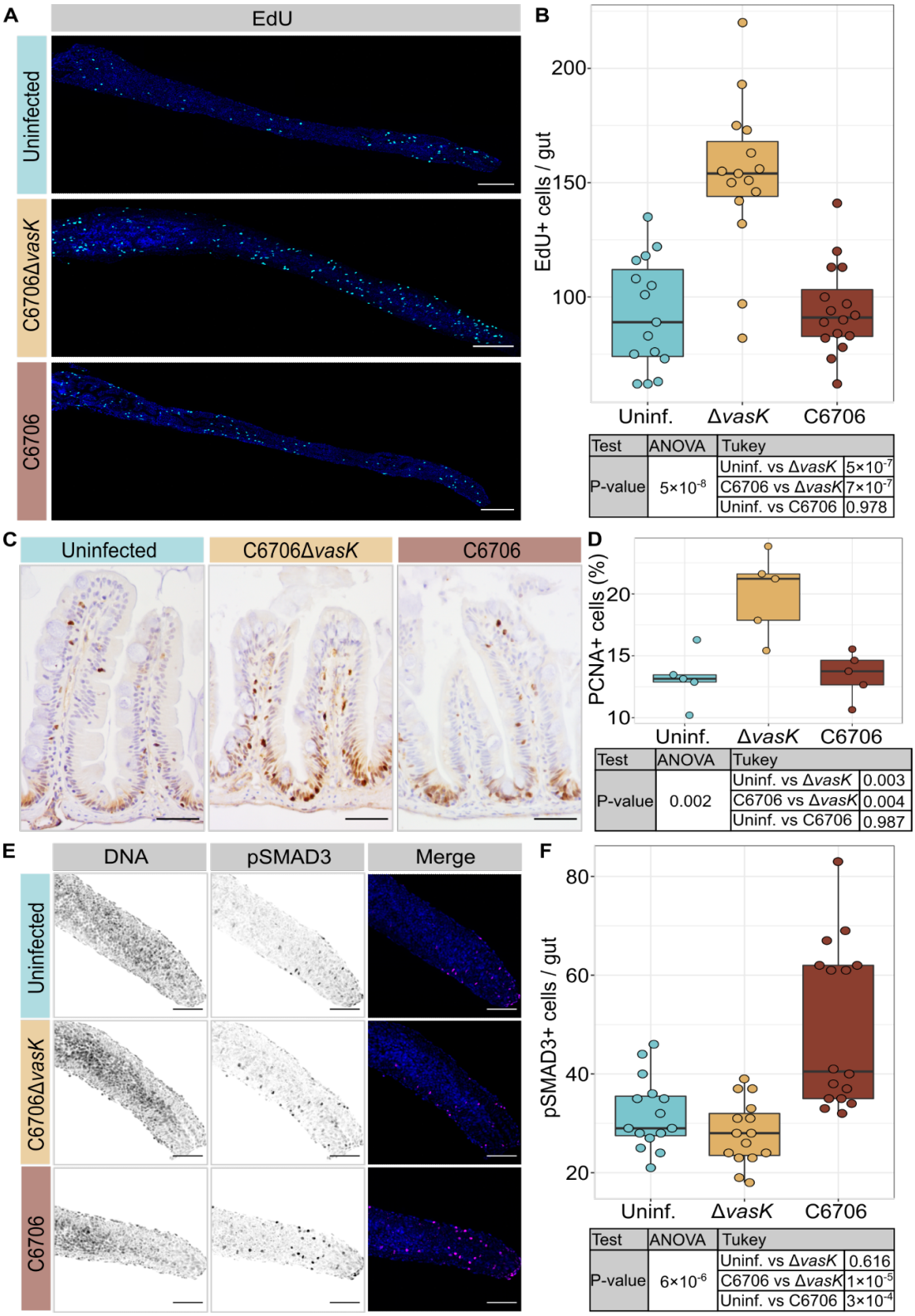

Figure 6. *Vc* T6SS induces BMP activation and limits cell proliferation in the zebrafish intestine. (A) Intestines of uninfected or *Vc*-infected TL zebrafish larvae with DNA stained by Hoechst in blue and EdU+ cells in cyan. Scale bars = 200 µm. **(B)** Quantification of EdU+ cells per gut. Each dot represents a

measurement from a single fish intestine. P values are calculated using the significance tests indicated in tables. **(C)** Immunohistochemical images of sagittal posterior intestinal sections from adult TL zebrafish stained for PCNA. Scale bars = 50 µm. **(D)** Percentage of intestinal epithelial cells that are PCNA+ in adult fish posterior intestine. Each dot represents a measurement from a single fish gut. **(E)** Posterior intestines from TL zebrafish larvae with DNA marked by Hoechst in blue and pSMAD3 in magenta. Scale bars = 100 µm. **(F)** Quantification of pSMAD3+ cells per gut with each dot representing a single gut.

DISCUSSION

Epithelial damage during enteric infection normally accelerates cell proliferation and tissue repair via stress responses such as the epidermal growth factor receptor (EGFR) and Janus kinase-signal transducer and activator of transcription (JAK-STAT) pathways[3–5,58]. However, oral infection of *Drosophila* with *Vc* leads to T6SS-dependent arrest of intestinal proliferation[26]. It is unknown how *Vc*-commensal interactions block epithelial repair. We consider this an important question, as failure to renew the intestinal epithelium exposes peri-intestinal tissue to gut-resident microbes, greatly increasing the risk of systemic infection. In this study, we found that interactions between *Vc* and host commensals activate BMP specifically in intestinal progenitor cells through the TNFR-like IMD pathway. BMP activity in EBs arrests ISC proliferation non-autonomously, which is necessary to block epithelial repair. Our study reveals how pathogen-commensal interactions engage evolutionarily conserved immune and growth regulators to impact epithelial renewal and also raises several interesting aspects to be further elucidated.

How does IMD activate intestinal BMP during a *Vc* infection? Normally, IMD serves a protective role and is essential for surviving infections by pathogens like *Pseudomonas entomophila*[59–61]. In contrast, *Vc*-dependent activation of IMD arrests ISC proliferation and severely shortens the host lifespan[18,19,23]. The precise mechanism by which *Vc* signals through the IMD pathway to disrupt gut epithelial barrier remains to be clarified. We found that *Vc*-commensal interactions activate BMP in progenitors via IMD signaling. IMD is typically activated by bacterial diaminopimelic acid-type peptidoglycan (DAP-PGN)[62–67], although alternate mechanisms also exist in the gut[68]. As fly symbiont *Acetobacter sp.* contain DAP-PGN and *Acetobacter pasteurianus* is sensitive to T6SS-dependent killing[19], we hypothesize that microbial components generated by T6SS-dependent killing of *Acetobacter sp.* initiate a signaling relay from IMD

to BMP. It seems likely that IMD is primarily activated in enterocytes during *Vc* infection, as these cells make direct contact with the intestinal lumen where they can detect DAP-PGN. Moreover, enterocyte-specific IMD activity plays a role in intestinal homeostasis, as deregulation of IMD in enterocytes induces progenitor hyperproliferation and dysplasia[69]. However, we cannot exclude the possibility that progenitor-specific IMD directly regulates BMP, as progenitors are capable of IMD responses[70–72], and microbial components may pass through the epithelial barrier and reach basally situated progenitors, especially with the presence of epithelial breaches caused by *Vc* infection[19]. Future studies should consider impacts of cell-type-specific innate defenses on epithelial renewal during enteric infections.

How does BMP regulate ISC proliferation? Mechanistically, our data suggest a non-autonomous role of BMP signaling in regulating epithelial renewal during infection. We found that *Vc*-responsive BMP activation in EBs blocks proliferation of neighboring ISCs. Our findings match an earlier report that EB-specific BMP inactivation stimulates ISC hyperproliferation upon challenges with *Ecc15* or in the absence of infection[41]. Currently, it is unclear how EB-specific BMP activity regulates ISC proliferation. Typically, epithelial damage during enteric infections enhance JAK-STAT and EGFR signals in ISCs, leading to an elevated proliferation rate[3–5,58]. A recent study suggested a functional link between BMP and stress responses in regulating intestinal epithelial renewal. Specifically, loss of BMP signals activated of JAK-STAT and EGFR signaling in fly midguts, which fueled stem cell division and eventually disrupted epithelial homeostasis[40]. Our previous transcriptional data showed that wildtype *Vc* did not initiate JAK-STAT and EGFR activity in midgut progenitors, whereas T6SS-deficient *Vc* successfully initiated both responses[26]. Thus, we speculate that BMP activity in EBs blocks epithelial proliferation by antagonizing JAK-STAT or EGFR responses in neighboring ISCs upon *Vc* infection. Further investigations are required to elucidate the mechanisms by which EB-specific BMP non-autonomously regulates stem cell growth during infections.

How does BMP regulate epithelial homeostasis during enteric infections? We found that T6SS-responsive activation of BMP blocks ISC proliferation, leading to an arrest of epithelial repair. Notably, our findings are not restricted to flies. *Vc* T6SS induces TGF-β/BMP activity in zebrafish intestines. Moreover, infection with *Vc* suppresses cell proliferation in a T6SS-dependent manner despite widespread damage to the fish intestinal epithelial barrier. It remains to be seen whether BMP signaling is necessary to block epithelial proliferation in the fish gut and whether the T6SS-responsive arrest of epithelial repair requires microbial interactions. Unlike fly guts which rely on germline-encoded innate defenses, zebrafish intestines also possess lymphocyte-based adaptive defenses that impact host responses to symbiotic and pathogenic microbes[57,73–78]. Recent studies reveal an immune-modulatory role of BMP in the vertebrate intestine[79–81]. In both human and mouse colon, epithelial-specific BMP activity limits expression of pro-inflammatory genes including a number of chemokines and cytokines and suppresses infiltration of macrophages and neutrophils[80,81]. Loss of the BMP pathway transcription factor SMAD4 in epithelial cells promotes inflammation-driven carcinogenesis in mouse colon[80,82]. Based on these findings and advantages of the zebrafish model, future studies could be conducted in fish to determine whether epithelial BMP signaling synergizes with innate and adaptive defenses to regulate the intestinal epithelial barrier during *Vc* infection. In addition to controlling cell proliferation and immune responses, intestinal BMP also regulates differentiation of immature intestinal epithelial cells in flies and vertebrates[38,45,83,84]. Therefore, it is possible that *Vc*-responsive BMP activation also impacts regeneration of a mature intestinal epithelium upon infection. Further investigations are needed to precisely determine roles of epithelial-specific BMP activity during enteric infections and how gut symbiotic and pathogenic microbes affect host responses.

In summary, this study demonstrates that *Vc*-commensal interactions modify host immune and growth regulatory pathways to disrupt intestinal epithelial repair. Using a *Drosophila* model, we uncovered

effects of BMP activity and innate defenses on epithelial renewal upon infection with *Vc*. Given the importance of BMP and TNFR-like signaling in regulating intestinal homeostasis, we consider this work relevant to understand how evolutionarily conserved pathways orchestrate host responses to a global health threat.

ACKNOWLEDGEMENTS

We are grateful to Bloomington Drosophila Stock Center, Dr. Bruce Edgar, Dr. Bruno Lemaitre, and Dr. Minjeong Shin for providing fly lines. *V. cholerae* C6706 was provided by Dr. John Mekalanos. We would also like to thank Science Animal Support Services and the Alberta Health Sciences Animal Laboratory Services for their excellent care of the zebrafish aquatic facilities. We acknowledge microscopy support from Dr. Steven Ogg, Gregory Plummer, and Kiera Smith at the Faculty of Medicine and Dentistry Cell Imaging Core. We acknowledge TEM support from Sara Amidian and Dr. Xuejun Sun at the Department of Oncology Cell Imaging Facility. We acknowledge the immunohistochemistry support provided by Dr. Kacie Norton at the Department of Biological Sciences Advanced Microscopy Facility and help from Mckenna Eklund. Thanks to Dr. Robert Ingham, Lena Jones, Mckenna Eklund, Aurélia Joly and Ralph Derrick De Leon for critical reading of the manuscript. This work was supported by a grant from the Canadian Institutes of Health Research to E.F. (MOP77746). X.X. has funding support through Alberta Graduate Excellence Scholarship and Li Ka Shing Institute of Virology Graduate Studies Entrance Award.

MATERIALS AND METHODS

Fly and zebrafish husbandry

Fly stocks and crosses were maintained at 18°C on standard cornmeal medium (Nutri-Fly Bloomington formulation https://bdsc-indianaedu.login.ezproxy.library.ualberta.ca/information/recipes/bloomfood.html). All experimental flies were virgin females kept at 18°C during collection and shifted to 29°C with a 12 hour/12 hour light/dark cycle to induce expression of transgenes of interest. Fly lines used in this study include *imd*^{EY08573} *(imd-/-)*[85], *w;esg-GAL4,tubGAL80*^{ts}*,UAS-GFP (esg*^{ts}*)*[11], *w;Su(H)GBE-GAL4,UAS-GFP;ubi-GAL80*^{ts} *(Su(H)*^{ts}*)*[86], *UAS-shn RNAi* (VDRC #KK-105643), *UAS-tkv*^{CA} (Bloomington #36536), *40D-UAS* (control for VDRC KK lines, VDRC #60101). We used *w*^{1118} as a wild-type control to set up crosses with *esg*^{ts} and *Su(H)*^{ts} lines. The *imd* line was backcrossed into our wild-type *w*^{1118} background for eight generations prior to use. As *white* mutants showed impaired biological functions including stress response in flies, we generated a wild-type control in Figure3 for *imd-/-* by introducing the *w+* allele from *Oregon R* line into our *w*^{1118} via backcrossing for eight generations.

Zebrafish were raised and maintained following protocols approved by the Animal Care & Use Committees, Biosciences and Health Sciences at the University of Alberta, operating under the guidelines of the Canadian Council of Animal Care. Adult TL strain zebrafish were reared at the University of Alberta fish facility at 29°C under a 14-hour/10-hour light/dark cycle using standard zebrafish husbandry protocols. Zebrafish were fasted for 22 hours prior to infection. For larval analysis, TL zebrafish embryos were collected from breeding tanks and transferred to glass petri dishes with embryo media (15 mM NaCl, 1 mM $CaCl_2$•$2H_2O$, 1 mM MgSO4•$7H_2O$, 0.7 mM $NaHCO_3$, 0.5 mM KCl, 0.15 mM KH_2PO_4 and 0.05 mM Na_2HPO_4 in MiliQ water). Embryos were raised at 29°C under a 14-hour/10-hour light/dark cycle. 6 day-post-fertilization larvae were used for *Vc* infection.

Generation of germ-free flies

To generate germ-free (GF) flies, freshly eclosed female *esg*^{ts}*/+* flies were raised on autoclaved food with antibiotics (100µg/mL Ampicillin, 100µg/mL Neomycin, 50µg/mL Vancomycin dissolved in 50% ethanol, and 100µg/mL Neomycin dissolved in water) for 5 days at 25°C. To ensure sterility, two flies from each vial were homogenized in MRS broth and plated on MRS agar plates. Flies were considered GF if no visible colonies formed. Conventionally reared (CR) flies were fed autoclaved food without antibiotics for 5 days at 25°C. Both GF and CR flies were then transferred onto autoclaved food without antibiotics for 7 days at 29°C, flipping onto freshly prepared food every 2 days. The sterility of GF flies was confirmed by plating fly homogenate on MRS plates 1 day prior to *Vc* infection.

***Vc* oral infection**

Virgin female flies were kept at 29°C for 7 days prior to infection. *esg*^{ts}*>shn*^{RNAi} flies and their wild-type counterparts (*esg*^{ts}*/+*) were maintained at 18°C for 10 days and then shifted to 29°C for 3 days to minimize detrimental effects of prolonged BMP inactivation. For oral infection in flies, *Vc* C6706 and C6706Δ*vasK*[48] were grown on LB plates (0.5% NaCl, 0.5% yeast extract, 1% tryptone, 1.5% agar) supplemented with 100 µg/ml streptomycin (Sigma SLBK5521V) for 16-18 hours at 37°C. To prepare a *Vc* infection culture, single colonies were removed from the plate, suspended in LB broth, and diluted to a final OD600 of 0.125. Flies were starved for 2 hours at 29°C prior to infection. In each vial, 10-15 flies were placed onto one-third of a cotton plug soaked with 3 ml of LB broth (Uninfected) or *Vc* infection culture (C6706 or C6706Δ*vasK*). Vials were kept at 29°C with a 12 hour/12 hour light/ dark cycle for oral infection.

For *Vc* infection in zebrafish, a single colony of C6706 or C6706Δ*vasK* was suspended in LB broth with 100 µg/ml streptomycin and grown with aeration overnight at 37°C. *Vc* cells were washed twice with PBS and diluted to OD600 of 1. To infect fish larvae, 15-20 larvae (6 days post fertilization) were incubated in each well of a 6-well plate containing 20 µL infection culture (C6706 or C6706Δ*vasK*) or 20 µL PBS (Uninfected) in 4 mL embryo medium. For infection in adult fish, 5 female fish per treatment were incubated in a 400 mL beaker with 1 mL infection culture (C6706 or C6706Δ*vasK*) or 1 mL PBS (Uninfected) in 200 mL filter sterilized fish tank water. Fish were kept in a 29°C incubator with a 14-hour/10-hour light/ dark cycle during infection.

Immunofluorescence

Fly intestines were dissected in PBS, fixed in 8% formaldehyde in PBS for 20 minutes, washed in PBS with 0.2% Triton-X (PBST) for 30 minutes, and blocked in PBST with 3% bovine serum albumin (BSA) for 1 hour at room temperature. Guts were stained overnight at 4°C in PBST + 3% BSA with appropriate primary antibodies. The following day guts were washed in PBST and stained for 1 hour at room temperature with secondary antibodies and DNA stain (1/1000 Hoechst 33258; Invitrogen H3569) in PBST + 3% BSA. Guts were washed in PBST for 30 minutes at room temperature then in PBS overnight at 4°C.

Zebrafish larvae (6 day-post-fertilization) were incubated in embryo medium with 1% DMSO and 5 mM EdU (Invitrogen C10340) for 8 hours at 29°C and then infected with *Vc* for 24 hours. Fish intestines were dissected in PBS and fixed in 4% paraformaldehyde in PBS overnight at 4°C. Guts were washed three times with PBSTx (0.75% TritonX-100 and 0.02% NaN_3 in PBS), blocked for 1 hour in PBSTx + 3% BSA at room temperature, and stained with primary antibodies in blocking buffer overnight at 4°C. Guts were washed with PBSTx and then stained for 1 hour at room temperature with secondary antibodies

and nuclear stain (1/1000 Hoechst 33258; Invitrogen H3569), followed by rinse in PBSTx. EdU detection was performed by incubating guts in Click-iT® reaction cocktail (Invitrogen C10340) for 30 minutes at room temperature. Guts were washed in PBSTx followed by extra washing in PBS.

Fly and fish intestines were mounted on microscope slides using Flouromount™ (Sigma; F4680) and visualized with a spinning-disk confocal microscope (Olympus IX-81 motorised microscope base with Yokagawa CSU 10 spinning-disk scan-head). Images fly posterior midguts (R4/5) and entire zebrafish larvae guts were acquired using Perkin Elmer's Volocity software, and all quantifications were performed manually with Fiji software. PH3+ cells in the entire fly midgut were counted through the eyepiece of the microscope.

Primary antibody used in this study are chicken anti-GFP (1/2000; Invitrogen PA1-9533), rabbit anti-PH3 (1/1000; Milipore 06-570), rabbit anti-pSmad3 (1/200; Abcam ab52903), mouse anti-armadillo (1/100; DSHB N2 7A1), mouse anti-Delta (1/100; DSHB C594.9B), and mouse anti-perospero (1/100; DSHB MR1A). Secondary antibodies used are goat anti-chicken 488 (Invitrogen A11039), goat anti-rabbit 568 (Invitrogen A11011) and goat anti-mouse 647 (Invitrogen A21235) at a concentration of 1/1000.

Immunohistochemistry

Intestines from adult zebrafish were dissected and fixed in BT fixative (0.15 mM $CaCl_2$, 0.1 M PO_4, 4% sucrose, 4% paraformaldehyde in dH_2O) for 48 hours at 4°C. Guts were embedded in paraffin, sectioned into 5 µm slices, and collected on Superfrost Plus slides. Sections were deparaffinized with Toluene and rehydrated. Antigen unmasking was performed by boiling slides in 0.1 M sodium citrate buffer (pH 6) in a 98°C water bath for 20 minutes. Sections were incubated in 3% hydrogen peroxide, washed with PBSt (0.5% TritonX-100 in PBS), blocked with 10% normal goat serum in PBSt, and incubated with mouse anti-PCNA (1/20000; Sigma P8825) overnight at 4°C in humid chamber. Sections were washed three times

with PBSt and incubated in SignalStain® Boost Detection Reagent (HRP, Mouse; CST 8125P) for 30 minutes at room temperature. SignalStain® DAB Chromogen solution (CST 8059) was added onto each section for colorimetric detection. Slides were rinsed and counterstained with ¼-strength hematoxylin. All sections were dehydrated and mounted in Dpx. Images were captured using ZEISS AXIO A1 compound light microscope with SeBaCam 5.1MP camera, and qualifications were done using Fiji software.

Transmission electron microscopy

Fly posterior midguts were cut into 1 mm pieces and immediately placed into fixative (3% paraformaldehyde and 3% glutaraldehyde in 0.1 M cacodylate buffer with 0.1 M $CaCl_2$, pH 7.2). Tissue processing was performed at the Cell Imaging Facility at University of Alberta. The midgut sagittal sections from 5 flies per treatment were visualized using a JEOL 2100 transmission electron microscope.

SUPPLEMENTARY FIGURES

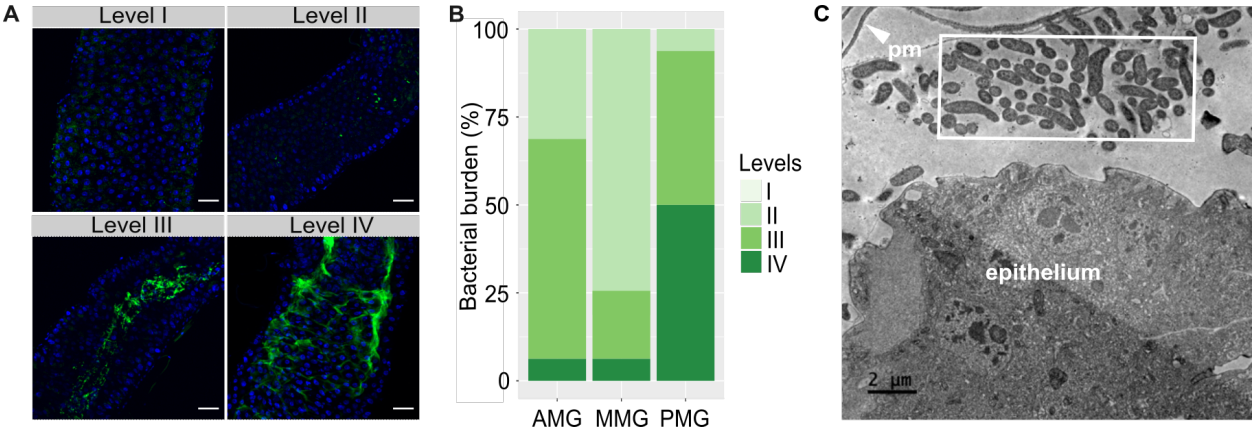

Supplementary Figure 1. *V. cholerae* colonize the posterior midgut of *Drosophila*.
(A) Immunofluorescence of fly midguts infected with C6706. DNA stained by Hoechst (blue) and GFP-labeled C6706 (green). Four different levels of bacterial burden: level I = no visible GFP-labeled bacteria, level II = a few scattered individual GFP-C6706, and large clumps of *V. cholerae* in the lumen (level III) or in close proximity to the intestinal epithelium (level IV). Scale bars = 25 µm. **(B)** Approximate bacterial burden in different regions of fly guts infected with C6706 (n=20) for 24 h. Assessment based on the four-level scale in (A). Anterior midgut, AMG; middle midgut, MMG; posterior midgut, PMG. **(C)** Transmission electron microscopy of the posterior midguts of flies infected with C6706 for 24 h. Clusters of rod-shaped *V. cholerae* are indicated with a white box. Peritrophic matrix, pm.

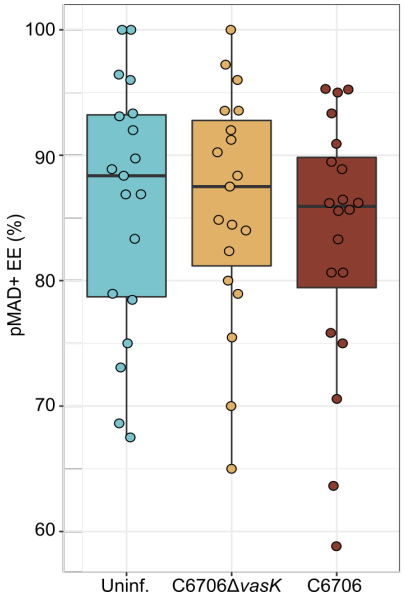

Test	ANOVA	Tukey	
P-value	0.601	Uninf. vs Δ*vasK*	0.999
		Uninf. vs C6706	0.649
		C6706 vs Δ*vasK*	0.669

Supplementary Figure 2. BMP activation in enteroendocrine cells.
Percentage of Pros+ enteroendocrine cells (EE) that are pMAD+ in uninfected guts, and gut infected with C6706Δ*vasK* or C6706. Each dot represents a measurement from a single fly gut. P values were calculated using the significance tests indicated in the table.

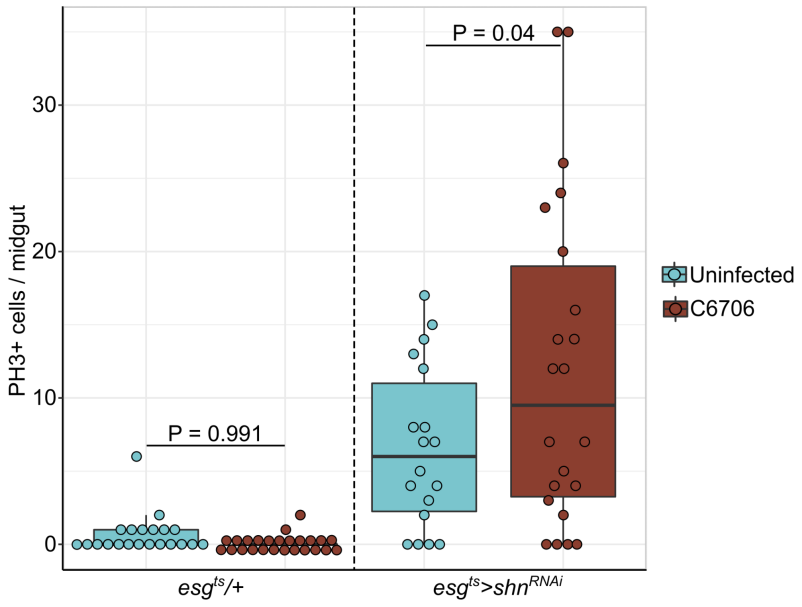

Supplementary Figure 3. BMP regulates cell proliferation after *Vc* infection. PH3+ cell per midgut in wild-type flies (*esg^{ts}/+*) or progenitor-specific shn knockdown flies (*esg^{ts}>shn^{RNAi}*) upon infection with C6706 for 36h. Each dot represents a measurement from a single fly gut. P values are calculated using unpaired Student t-tests.

REFERENCES

1. Amcheslavsky, A., Jiang, J. & Ip, Y. T. Tissue Damage-Induced Intestinal Stem Cell Division in Drosophila. *Cell Stem Cell* **4**, 49–61 (2009).
2. Buchon, N., Broderick, N. A., Poidevin, M., Pradervand, S. & Lemaitre, B. Drosophila Intestinal Response to Bacterial Infection: Activation of Host Defense and Stem Cell Proliferation. *Cell Host Microbe* **5**, 200–211 (2009).
3. Buchon, N., Broderick, N. A., Chakrabarti, S. & Lemaitre, B. Invasive and indigenous microbiota impact intestinal stem cell activity through multiple pathways in Drosophila. *Genes Dev.* **23**, 2333–2344 (2009).
4. Jiang, H. *et al.* Cytokine/Jak/Stat Signaling Mediates Regeneration and Homeostasis in the Drosophila Midgut. *Cell* **137**, 1343–1355 (2009).
5. Buchon, N., Broderick, N. A., Kuraishi, T. & Lemaitre, B. Drosophila EGFR pathway coordinates stem cell proliferation and gut remodeling following infection. *BMC Biol.* **8**, 152 (2010).
6. Ali, M., Nelson, A. R., Lopez, A. L. & Sack, D. A. Updated Global Burden of Cholera in Endemic Countries. *PLoS Negl. Trop. Dis.* **9**, e0003832 (2015).
7. Das, B., Verma, J., Kumar, P., Ghosh, A. & Ramamurthy, T. Antibiotic resistance in Vibrio cholerae: Understanding the ecology of resistance genes and mechanisms. *Vaccine* **38**, A83–A92 (2020).
8. Davoodi, S. & Foley, E. Host-Microbe-Pathogen Interactions: A Review of Vibrio cholerae Pathogenesis in Drosophila. *Front. Immunol.* **10**, (2020).
9. Echeverria, P., Harrison, B. A., Tirapat, C. & McFarland, A. Flies as a source of enteric pathogens in a rural village in Thailand. *Appl. Environ. Microbiol.* **46**, 32–36 (1983).
10. Fotedar, R. Vector potential of houseflies (Musca domestica) in the transmission of Vibrio cholerae in India. *Acta Trop.* **78**, 31–34 (2001).

11. Micchelli, C. A. & Perrimon, N. Evidence that stem cells reside in the adult Drosophila midgut epithelium. *Nature* **439**, 475–479 (2006).

12. Ohlstein, B. & Spradling, A. The adult Drosophila posterior midgut is maintained by pluripotent stem cells. *Nature* **439**, 470–474 (2006).

13. Casali, A. & Batlle, E. Intestinal Stem Cells in Mammals and Drosophila. *Cell Stem Cell* **4**, 124–127 (2009).

14. Jiang, H. & Edgar, B. A. Intestinal stem cells in the adult Drosophila midgut. *Exp. Cell Res.* **317**, 2780–2788 (2011).

15. Jiang, H. & Edgar, B. A. Intestinal stem cell function in Drosophila and mice. *Curr. Opin. Genet. Dev.* **22**, 354–360 (2012).

16. Buchon, N. *et al.* Morphological and Molecular Characterization of Adult Midgut Compartmentalization in Drosophila. *Cell Rep.* **3**, 1725–1738 (2013).

17. Blow, N. S. *et al.* Vibrio cholerae Infection of Drosophila melanogaster Mimics the Human Disease Cholera. *PLoS Pathog.* **1**, e8 (2005).

18. Berkey, C. D., Blow, N. & Watnick, P. I. Genetic analysis of Drosophila melanogaster susceptibility to intestinal Vibrio cholerae infection. *Cell. Microbiol.* **11**, 461–474 (2009).

19. Fast, D., Kostiuk, B., Foley, E. & Pukatzki, S. Commensal pathogen competition impacts host viability. *Proc. Natl. Acad. Sci.* **115**, 7099–7104 (2018).

20. Anderson, A. M. L. *et al.* Non-o1 Vibrio cholerae septicemia: Case report, discussion of literature, and relevance to bioterrorism. *Diagn. Microbiol. Infect. Dis.* **49**, 295–297 (2004).

21. Purdy, A. E. & Watnick, P. I. Spatially selective colonization of the arthropod intestine through activation of Vibrio cholerae biofilm formation. *Proc. Natl. Acad. Sci.* **108**, 19737–19742 (2011).

22. Guichard, A. *et al.* Cholera Toxin Disrupts Barrier Function by Inhibiting Exocyst-Mediated Trafficking of Host Proteins to Intestinal Cell Junctions. *Cell Host Microbe* **14**, 294–305 (2013).

23. Wang, Z., Hang, S., Purdy, A. E. & Watnick, P. I. Mutations in the IMD Pathway and Mustard Counter Vibrio cholerae Suppression of Intestinal Stem Cell Division in Drosophila. *mBio* **4**, e00337-13 (2013).

24. Kleino, A. & Silverman, N. The Drosophila IMD pathway in the activation of the humoral immune response. *Dev. Comp. Immunol.* **42**, 10.1016/j.dci.2013.05.014 (2014).

25. Myllymäki, H., Valanne, S. & Rämet, M. The Drosophila imd signaling pathway. *J. Immunol. Baltim. Md 1950* **192**, 3455–3462 (2014).

26. Fast, D. *et al.* Vibrio cholerae-Symbiont Interactions Inhibit Intestinal Repair in Drosophila. *Cell Rep.* **30**, 1088-1100.e5 (2020).

27. Mougous, J. D. *et al.* A Virulence Locus of Pseudomonas aeruginosa Encodes a Protein Secretion Apparatus. *Science* **312**, 1526–1530 (2006).

28. Pukatzki, S., Ma, A. T., Revel, A. T., Sturtevant, D. & Mekalanos, J. J. Type VI secretion system translocates a phage tail spike-like protein into target cells where it cross-links actin. *Proc. Natl. Acad. Sci.* **104**, 15508–15513 (2007).

29. MacIntyre, D. L., Miyata, S. T., Kitaoka, M. & Pukatzki, S. The Vibrio cholerae type VI secretion system displays antimicrobial properties. *Proc. Natl. Acad. Sci.* **107**, 19520–19524 (2010).

30. Basler, M., Pilhofer, M., Henderson, G. P., Jensen, G. J. & Mekalanos, J. J. Type VI secretion requires a dynamic contractile phage tail-like structure. *Nature* **483**, 182–186 (2012).

31. Pukatzki, S., McAuley, S. B. & Miyata, S. T. The type VI secretion system: translocation of effectors and effector-domains. *Curr. Opin. Microbiol.* **12**, 11–17 (2009).

32. Schwarz, S. *et al.* Burkholderia Type VI Secretion Systems Have Distinct Roles in Eukaryotic and Bacterial Cell Interactions. *PLOS Pathog.* **6**, e1001068 (2010).

33. Serapio-Palacios, A. *et al.* Type VI secretion systems of pathogenic and commensal bacteria mediate niche occupancy in the gut. *Cell Rep.* **39**, 110731 (2022).

34. Ma, A. T. & Mekalanos, J. J. In vivo actin cross-linking induced by Vibrio cholerae type VI secretion system is associated with intestinal inflammation. *Proc. Natl. Acad. Sci.* **107**, 4365–4370 (2010).

35. Zhao, W., Caro, F., Robins, W. & Mekalanos, J. J. Antagonism toward the intestinal microbiota and its effect on Vibrio cholerae virulence. *Science* **359**, 210–213 (2018).

36. Haramis, A.-P. G. *et al.* De Novo Crypt Formation and Juvenile Polyposis on BMP Inhibition in Mouse Intestine. *Science* **303**, 1684–1686 (2004).

37. He, X. C. *et al.* BMP signaling inhibits intestinal stem cell self-renewal through suppression of Wnt–β-catenin signaling. *Nat. Genet.* **36**, 1117–1121 (2004).

38. Auclair, B. A., Benoit, Y. D., Rivard, N., Mishina, Y. & Perreault, N. Bone Morphogenetic Protein Signaling Is Essential for Terminal Differentiation of the Intestinal Secretory Cell Lineage. *Gastroenterology* **133**, 887–896 (2007).

39. Guo, Z., Driver, I. & Ohlstein, B. Injury-induced BMP signaling negatively regulates Drosophila midgut homeostasis. *J. Cell Biol.* **201**, 945–961 (2013).

40. Li, Z., Zhang, Y., Han, L., Shi, L. & Lin, X. Trachea-Derived Dpp Controls Adult Midgut Homeostasis in Drosophila. *Dev. Cell* **24**, 133–143 (2013).

41. Zhou, J. *et al.* Dpp/Gbb signaling is required for normal intestinal regeneration during infection. *Dev. Biol.* **399**, 189–203 (2015).

42. Walton, K. D. *et al.* Villification in the mouse: Bmp signals control intestinal villus patterning. *Dev. Camb. Engl.* **143**, 427–436 (2016).

43. Múnera, J. O. *et al.* Differentiation of Human Pluripotent Stem Cells into Colonic Organoids via Transient Activation of BMP Signaling. *Cell Stem Cell* **21**, 51-64.e6 (2017).

44. Tian, A., Wang, B. & Jiang, J. Injury-stimulated and self-restrained BMP signaling dynamically regulates stem cell pool size during *Drosophila* midgut regeneration. *Proc. Natl. Acad. Sci.* **114**, (2017).

45. Zhang, Y. & Que, J. BMP Signaling in Development, Stem Cells, and Diseases of the Gastrointestinal Tract. *Annu. Rev. Physiol.* **82**, 251–273 (2020).

46. Zhou, J. & Boutros, M. JNK-dependent intestinal barrier failure disrupts host–microbe homeostasis during tumorigenesis. *Proc. Natl. Acad. Sci.* **117**, 9401–9412 (2020).

47. Zhou, J., Valentini, E. & Boutros, M. Microenvironmental innate immune signaling and cell mechanical responses promote tumor growth. *Dev. Cell* **56**, 1884-1899.e5 (2021).

48. Pukatzki, S. *et al.* Identification of a conserved bacterial protein secretion system in Vibrio cholerae using the Dictyostelium host model system. *Proc. Natl. Acad. Sci.* **103**, 1528–1533 (2006).

49. Broderick, N. A., Buchon, N. & Lemaitre, B. Microbiota-Induced Changes in Drosophila melanogaster Host Gene Expression and Gut Morphology. *mBio* **5**, e01117-14 (2014).

50. Runft, D. L. *et al.* Zebrafish as a Natural Host Model for Vibrio cholerae Colonization and Transmission. *Appl. Environ. Microbiol.* **80**, 1710–1717 (2014).

51. Mitchell, K. C. & Withey, J. H. Danio rerio as a Native Host Model for Understanding Pathophysiology of Vibrio cholerae. *Methods Mol. Biol. Clifton NJ* **1839**, 97–102 (2018).

52. Nag, D., Farr, D. A., Walton, M. G. & Withey, J. H. Zebrafish Models for Pathogenic Vibrios. *J. Bacteriol.* **202**, e00165-20 (2020).

53. Senderovich, Y., Izhaki, I. & Halpern, M. Fish as Reservoirs and Vectors of Vibrio cholerae. *PLoS ONE* **5**, e8607 (2010).

54. Halpern, M. & Izhaki, I. Fish as Hosts of Vibrio cholerae. *Front. Microbiol.* **8**, 282 (2017).

55. Nag, D., Mitchell, K., Breen, P. & Withey, J. H. Quantifying Vibrio cholerae Colonization and Diarrhea in the Adult Zebrafish Model. *J. Vis. Exp. JoVE* 57767 (2018).

56. Wallace, K. N., Akhter, S., Smith, E. M., Lorent, K. & Pack, M. Intestinal growth and differentiation in zebrafish. *Mech. Dev.* **122**, 157–173 (2005).

57. Flores, E. M., Nguyen, A. T., Odem, M. A., Eisenhoffer, G. T. & Krachler, A. M. The Zebrafish as a Model for Gastrointestinal Tract - Microbe Interactions. *Cell. Microbiol.* **22**, e13152 (2020).

58. Jiang, H., Grenley, M. O., Bravo, M.-J., Blumhagen, R. Z. & Edgar, B. A. EGFR/Ras/MAPK Signaling Mediates Adult Midgut Epithelial Homeostasis and Regeneration in Drosophila. *Cell Stem Cell* **8**, 84–95 (2011).

59. Vodovar, N. *et al.* Drosophila host defense after oral infection by an entomopathogenic Pseudomonas species. *Proc. Natl. Acad. Sci. U. S. A.* **102**, 11414–11419 (2005).

60. Liehl, P., Blight, M., Vodovar, N., Boccard, F. & Lemaitre, B. Prevalence of Local Immune Response against Oral Infection in a Drosophila/Pseudomonas Infection Model. *PLoS Pathog.* **2**, e56 (2006).

61. Nehme, N. T. *et al.* A Model of Bacterial Intestinal Infections in Drosophila melanogaster. *PLoS Pathog.* **3**, e173 (2007).

62. Leulier, F. *et al.* The Drosophila immune system detects bacteria through specific peptidoglycan recognition. *Nat. Immunol.* **4**, 478–484 (2003).

63. Werner, T., Borge-Renberg, K., Mellroth, P., Steiner, H. & Hultmark, D. Functional Diversity of the Drosophila PGRP-LC Gene Cluster in the Response to Lipopolysaccharide and Peptidoglycan*. *J. Biol. Chem.* **278**, 26319–26322 (2003).

64. Kaneko, T. *et al.* Monomeric and Polymeric Gram-Negative Peptidoglycan but Not Purified LPS Stimulate the Drosophila IMD Pathway. *Immunity* **20**, 637–649 (2004).

65. Stenbak, C. R. *et al.* Peptidoglycan Molecular Requirements Allowing Detection by the Drosophila Immune Deficiency Pathway1. *J. Immunol.* **173**, 7339–7348 (2004).

66. Takehana, A. *et al.* Peptidoglycan recognition protein (PGRP)-LE and PGRP-LC act synergistically in Drosophila immunity. *EMBO J.* **23**, 4690–4700 (2004).

67. Bosco-Drayon, V. *et al.* Peptidoglycan Sensing by the Receptor PGRP-LE in the Drosophila Gut Induces Immune Responses to Infectious Bacteria and Tolerance to Microbiota. *Cell Host Microbe* **12**, 153–165 (2012).

68. Kamareddine, L., Robins, W. P., Berkey, C. D., Mekalanos, J. J. & Watnick, P. I. The Drosophila Immune Deficiency Pathway Modulates Enteroendocrine Function and Host Metabolism. *Cell Metab.* **28**, 449-462.e5 (2018).

69. Zhai, Z., Boquete, J.-P. & Lemaitre, B. Cell-Specific Imd-NF-κB Responses Enable Simultaneous Antibacterial Immunity and Intestinal Epithelial Cell Shedding upon Bacterial Infection. *Immunity* **48**, 897-910.e7 (2018).

70. Petkau, K., Ferguson, M., Guntermann, S. & Foley, E. Constitutive Immune Activity Promotes Tumorigenesis in Drosophila Intestinal Progenitor Cells. *Cell Rep.* **20**, 1784–1793 (2017).

71. Liu, X. *et al.* Microbes affect gut epithelial cell composition through immune-dependent regulation of intestinal stem cell differentiation. *Cell Rep.* **38**, 110572 (2022).

72. Shin, M. *et al.* Immune regulation of intestinal-stem-cell function in Drosophila. *Stem Cell Rep.* **17**, 741–755 (2022).

73. Boehm, T., Bleul, C. C. & Schorpp, M. Genetic dissection of thymus development in mouse and zebrafish. *Immunol. Rev.* **195**, 15–27 (2003).

74. Lewis, K. L., Del Cid, N. & Traver, D. Perspectives on antigen presenting cells in zebrafish. *Dev. Comp. Immunol.* **46**, 63–73 (2014).

75. Zhu, L. *et al.* B Cells in Teleost Fish Act as Pivotal Initiating APCs in Priming Adaptive Immunity: An Evolutionary Perspective on the Origin of the B-1 Cell Subset and B7 Molecules. *J. Immunol.* **192**, 2699–2714 (2014).

76. Brugman, S. The zebrafish as a model to study intestinal inflammation. *Dev. Comp. Immunol.* **64**, 82–92 (2016).

77. Jung, H. M. *et al.* Development of the larval lymphatic system in zebrafish. *Dev. Camb. Engl.* **144**, 2070–2081 (2017).

78. Willms, R. J., Jones, L. O., Hocking, J. C. & Foley, E. A cell atlas of microbe-responsive processes in the zebrafish intestine. *Cell Rep.* **38**, 110311 (2022).

79. Kim, B.-G. *et al.* Smad4 signalling in T cells is required for suppression of gastrointestinal cancer. *Nature* **441**, 1015–1019 (2006).

80. Means, A. L. *et al.* Epithelial Smad4 Deletion Up-Regulates Inflammation and Promotes Inflammation-Associated Cancer. *Cell. Mol. Gastroenterol. Hepatol.* **6**, 257–276 (2018).

81. Lindholm, H. T. *et al.* BMP signaling in the intestinal epithelium drives a critical feedback loop to restrain IL-13–driven tuft cell hyperplasia. *Sci. Immunol.* **7**, eabl6543 (2022).

82. Liu, L. *et al.* Transforming Growth Factor Beta Promotes Inflammation and Tumorigenesis in Smad4-Deficient Intestinal Epithelium in a YAP-Dependent Manner. *Adv. Sci.* **n/a**, (2023).

83. Beumer, J. *et al.* Enteroendocrine cells switch hormone expression along the crypt-to-villus BMP signaling gradient. *Nat. Cell Biol.* **20**, 909–916 (2018).

84. Beumer, J. *et al.* BMP gradient along the intestinal villus axis controls zonated enterocyte and goblet cell states. *Cell Rep.* **38**, 110438 (2022).

85. Avadhanula, V., Weasner, B. P., Hardy, G. G., Kumar, J. P. & Hardy, R. W. A Novel System for the Launch of Alphavirus RNA Synthesis Reveals a Role for the Imd Pathway in Arthropod Antiviral Response. *PLOS Pathog.* **5**, e1000582 (2009).

86. Zeng, X., Chauhan, C. & Hou, S. X. Characterization of Midgut Stem Cell– and Enteroblast-Specific Gal4 Lines in Drosophila. *Genes. N. Y. N 2000* **48**, 607–611 (2010).